

Redistribution of the tight junction protein ZO-1 during physiological shedding of mouse intestinal epithelial cells

Yanfang Guan, Alastair J. M. Watson, Amanda M. Marchiando, Emily Bradford, Le Shen, Jerrold R. Turner and Marshall H. Montrose

Am J Physiol Cell Physiol 300:C1404-C1414, 2011. First published 23 February 2011;
doi:10.1152/ajpcell.00270.2010

You might find this additional info useful...

Supplemental material for this article can be found at:

<http://ajpcell.physiology.org/content/suppl/2011/03/02/ajpcell.00270.2010.DC1.html>

This article cites 30 articles, 12 of which can be accessed free at:

<http://ajpcell.physiology.org/content/300/6/C1404.full.html#ref-list-1>

Updated information and services including high resolution figures, can be found at:

<http://ajpcell.physiology.org/content/300/6/C1404.full.html>

Additional material and information about *AJP - Cell Physiology* can be found at:

<http://www.the-aps.org/publications/ajpcell>

This information is current as of June 16, 2011.

Redistribution of the tight junction protein ZO-1 during physiological shedding of mouse intestinal epithelial cells

Yanfang Guan,¹ Alastair J. M. Watson,² Amanda M. Marchiando,³ Emily Bradford,³ Le Shen,³ Jerrold R. Turner,³ and Marshall H. Montrose¹

¹Department of Molecular and Cellular Physiology, University of Cincinnati, Cincinnati, Ohio; ²Department of Translational Medicine, Norwich Medical School, University of East Anglia, Norwich, United Kingdom; and ³Department of Pathology, University of Chicago, Chicago, Illinois

Submitted 9 July 2010; accepted in final form 18 February 2011

Guan Y, Watson AJ, Marchiando AM, Bradford E, Shen L, Turner JR, Montrose MH. Redistribution of the tight junction protein ZO-1 during physiological shedding of mouse intestinal epithelial cells. *Am J Physiol Cell Physiol* 300: C1404–C1414, 2011. First published February 23, 2011; doi:10.1152/ajpcell.00270.2010.—We questioned how tight junctions contribute to intestinal barrier function during the cell shedding that is part of physiological cell renewal. Intravital confocal microscopy studied the jejunal villus epithelium of mice expressing a fluorescent zonula occludens 1 (ZO-1) fusion protein. Vital staining also visualized the cell nucleus (Hoechst staining) or local permeability to luminal constituents (Lucifer Yellow; LY). In a cell fated to be shed, ZO-1 redistributes from the tight junction toward the apical and then basolateral cell region. ZO-1 rearrangement occurs 15 ± 6 min ($n = 28$) before movement of the cell nucleus from the epithelial layer. During cell extrusion, permeation of luminal LY extends along the lateral intercellular spaces of the shedding cell only as far as the location of ZO-1. Within 3 min after detachment from the epithelial layer, nuclear chromatin condenses. After cell loss, a residual patch of ZO-1 remains in the space previously occupied by the departed cell, and the size of the patch shrinks to $14 \pm 2\%$ ($n = 15$) of the original cell space over 20 min. The duration of cell shedding measured by nucleus movement (14 ± 1 min) is much less than the total duration of ZO-1 redistribution at the same sites (45 ± 2 min). In about 15% of cell shedding cases, neighboring epithelial cells also undergo extrusion with a delay of 5–10 min. With the use of normal mice, ZO-1 immunofluorescent staining of fixed tissue confirmed ZO-1 redistribution and the presence of ZO-1 patches beneath shedding cells. Immunostaining also showed that redistribution of ZO-1 occurred without corresponding mixing of apical and basolateral membrane domains as marked by ezrin or E-cadherin. ZO-1 redistribution is the earliest cellular event yet identified as a herald of physiological cell shedding, and redistribution of tight junction function along the lateral plasma membrane sustains epithelial barrier during cell shedding.

jejunum; fluorescent protein; intestinal permeability; intravital microscopy; laser scanning confocal microscopy; multiphoton microscopy

THE EPITHELIUM of the small intestine functions as a selective barrier, protecting the organism against penetration by harmful agents (34). In part because of the intense and continuous interactions between the epithelium and the luminal environment, the epithelium has evolved to undergo rapid turnover, where cells are extruded frequently from the villus and replaced by others (14, 17, 23, 35). Cell extrusion successfully

maintains epithelial barrier function, even during cell loss, by some mechanism that is still poorly understood (3, 10, 18–20, 35–37). This mechanism even appears to maintain barrier function at transient discontinuities in the intestinal epithelium. Such “gaps” (defined as a lack of an intravital stained cell nucleus in the epithelial layer) can result from cell shedding and have also been observed in the steady-state census of cell positions on the villus epithelium (3, 16, 35–37).

Tight junctions prevent diffusion of molecules between adjacent epithelial cells and confer epithelial tightness, but their role during physiological cell shedding is unclear. These junctions are highly dynamic structures consisting of numerous interacting proteins (28). Clearly, cell shedding requires alterations in tight junction configuration. Electron microscopy has suggested that the junctions rearrange beneath dividing and shedding cells to maintain epithelial barrier function by connecting the cells neighboring an extruding cell (1, 3, 15, 37). Studies in which cell renewal was stimulated experimentally have provided some insight into the interplay between tight junction proteins and the maintenance of epithelial barrier function. Tumor necrosis factor- α (TNF- α) stimulates epithelial cell shedding nearly 30-fold (16), enhances caveolin-1-dependent endocytosis of the transmembrane tight junction protein occludin, and compromises tight junction barrier function (20). In other studies, experimentally induced epithelial wounds cause F-actin and myosin-II to accumulate at tight junctions and form a “purse-string” that closes the wound to restore epithelial barrier function (2, 5). Phosphorylated myosin light chain has been observed at sites of physiological cell shedding (3, 33) and in inflammatory bowel disease tissues (4, 26), suggesting that tight junction regulation is likely impacted during cell extrusion. Intriguingly, the tight junction scaffold protein, zonula occludens protein-1 (ZO-1), recently shown to render structural firmness and impermeability to the junction, is a link between occludin and the actin cytoskeleton (7, 8, 24). Therefore, ZO-1 may play a role in physiological epithelial cell extrusion and subsequent barrier maintenance.

Using a transgenic mouse expressing a fusion protein between monomeric red fluorescent protein (mRFP1) and ZO-1 (20), intravital staining (12, 16) and immunofluorescence, we have examined the subcellular redistribution of ZO-1 while directly visualizing physiological cell shedding without pharmacological or mechanical stimulation. As a result, we here report for the first time the three-dimensional and temporal dynamics of physiological cell extrusion in relation to epithelial barrier function in the intestine. Our observations support a model where tight junction reorganization allows for intestinal epithelial cell renewal without loss of barrier function.

Address for reprint requests and other correspondence: M. H. Montrose, Dept. of Molecular and Cellular Physiology, ML0576, Univ. of Cincinnati College of Medicine, 231 Albert Sabin Way, Cincinnati, OH 45267-0576 (e-mail: mhm@uc.edu).

MATERIALS AND METHODS

Animals. We used wild-type mice or transgenic mice expressing a fluorescent fusion protein (mRFP1 linked to the amino terminus of the tight junction protein ZO-1, under the control of the 9-kb villin promoter), on a C57BL/6 genetic background (for details, see Refs. 20 and 27). Breeding colonies in our Chicago and Cincinnati laboratories were group-housed and kept on a 12:12 h light-dark cycle (lights off: 7:00 p.m.), with constant access to standard rodent diet and water. Protocols were approved by the Animal Care and Use Committees at the University of Chicago and the University of Cincinnati.

Surgical preparation. Mice (age ~12 wk) were surgically prepared for imaging of the exposed small intestinal villi, by modification of previous procedures (12), as summarized below. They were anesthetized by intraperitoneal injection of ketamine hydrochloride (50 mg/kg body wt; Ketaject, Phoenix Scientific, St. Joseph, MO) and thiobutyl barbital (120 mg/kg body wt; Inactin; Sigma Chemical, St. Louis, MO). The nuclear dyes Hoechst 33342 or Hoechst 33258 (2 mg/kg body wt; Invitrogen, Eugene, OR) were injected via the tail vein. The abdomen was opened by a midline incision, and ~1.5 cm of jejunum was exteriorized. Peristalsis of the intestine was reduced by topical application of ~50 μ l 2% xylazine (Ben Venue Laboratories, Bedford, OH). The intestine was slit open at the anti-mesenteric side by electrocauterization, and the gut segment was rinsed with saline. The animal was placed in a dark, temperature-controlled (37°C) box on the stage of an inverted LSM 510 NLO microscope (Carl Zeiss, Jena, Germany), with the exposed mucosa facing the $\times 40$ objective lens. The mucosal surface was constantly superfused at 0.2 ml/min (KD Scientific push/pull syringe pump; Holliston, MA) with medium containing (in mM) 130 NaCl, 5 KCl, 1 MgSO₄, 2 CaCl₂, 1 Na₂HPO₄, 20 HEPES, and 25 mannose; pH 7.4. In some studies, 50 μ M Lucifer Yellow (LY, CH lithium salt; Molecular Probes, Eugene, OR) was added to the medium to monitor villus epithelial permeability.

In vivo imaging. Confocal fluorescence was recorded for mRFP1 [excitation (EX) 543 nm, emission (EM) 565–615 nm, optical section thickness 2.1 μ m] or for LY (EX 458 nm, EM 500–550 nm, optical section thickness 1.2 μ m). Nucleus staining with Hoechst was studied by two-photon microscopy (EX 730 nm, EM 435–485 nm). In time-course experiments, fluorescence images of epithelial cells were recorded near the tip of small intestinal villi at 4-min intervals. At each time point, a set of five XY-plane images were taken at 5- μ m focus intervals (1,024 \times 1,024 pixels recording of 230 μ m \times 230 μ m tissue area in each image). For higher three-dimensional resolution of more static structures, 20 XY-plane images were collected at 0.5- μ m focus intervals.

Immunocytochemistry. Immunostaining and imaging of stained sections were performed precisely as described before (32). Briefly, frozen sections of normal mouse jejunum were fixed in 1% paraformaldehyde and immunostained using anti-ZO-1 (rat or mouse monoclonal, Invitrogen), anti- β -actin, anti-ezrin (mouse monoclonal, Sigma), and anti-E-cadherin (rat-anti-mouse, Invitrogen), followed by Alexa Fluor 594- or 488-conjugated secondary antisera (Invitrogen), respectively. Cell nuclei were stained by incubating sections in Hoechst 33342 (37). Stained sections were imaged with a $\times 63$, 1.32 numerical aperture oil immersion objective on a DM4000 epifluorescence microscope (Leica, Wetzlar, Germany) and a CoolSNAP HQ camera (Roper Industries, Houston, TX). Z-stacks were collected at 0.2- μ m intervals and deconvolved using AutoDeblur (version X1; Media Cybernetics, Bethesda, MD) with 10 iterations.

Image analysis and statistics. Our confocal image collection strategy was designed to compensate for tissue movement due to intestinal smooth muscle contraction, which was minimized (but not fully eliminated) by xylazine, and for heartbeat and breathing artifacts. Lateral motion of tissue was compensated by examining a large image area at high-pixel resolution, and movement along the focal axis was compensated by selecting similar tissue regions from the multiple planes of focus collected at each time point. In this way, we could

monitor the dynamic process of individual cell movement and shedding for periods up to 2 h. Postacquisition image analysis was performed with MetaMorph and ImageJ (NIH, Bethesda, MD) software. Sizes of cells, their nuclei, and epithelial gaps were characterized by measuring their diameter and perimeter. Fluorescence intensity of structures was assessed using background-corrected 8-bit images by measuring the mean intensity value from relevant areas and normalizing values to results from the same structure at the start of experimentation. Data were expressed as means \pm SE of multiple experiments. Means were compared with Student's *t*-test or analysis of variance (the latter including Bonferroni's post hoc test), as appropriate (Prism; GraphPad Software, San Diego, CA) ($\alpha = 5\%$) (30).

RESULTS

Our goal was to determine how the rearrangement of tight junctions affects tissue permeability during cell shedding that mediates the physiological renewal of the small intestinal epithelium. We used intravital confocal and two-photon microscopy to examine the jejunal villus epithelium at high resolution in anesthetized mice, as described previously (11, 12). Four fluorescent markers, applied in suitable combinations, were used to follow the process: Hoechst 33342 or Hoechst 33258 to label the cell nucleus, a transgene expressing an mRFP1-ZO-1 fusion protein to track the tight junction protein ZO-1, and LY to label luminal perfusate and thereby monitor local changes in epithelial permeability.

Dynamic ZO-1 redistribution before and during cell shedding. Figure 1 shows in vivo images of the living villus epithelium, in which animals expressing the mRFP1-ZO-1 fusion protein also had the cell nucleus labeled with Hoechst 33342. The figure presents a set of five images collected along the focal axis at 5- μ m intervals. The imaging area usually included 2–4 cross-sectioned villi (V in Fig. 1A) and the luminal intervillous space (L in Fig. 1A) between them. On average, 2–8 cell shedding events could be observed in such an area during 90 min. As shown, the highest expression of the fluorescent ZO-1 is at the most luminal portion of epithelial lateral plasma membranes, where tight junctions interconnect epithelial cells. This can be observed in en face view at the luminal surface of epithelial villus cells (Fig. 1A) as well as in en profile view where cells are imaged directly along the apical-to-basal axis (Fig. 1, B–E).

Figure 2A shows a representative time course of physiological cell shedding in en profile images collected during intravital imaging and highlighting a cell that undergoes extrusion during observation (yellow circle). As the first sign of this process, ZO-1 shows condensation at the tight junctions, and part of the ZO-1 becomes detached from the junctions and accumulates in the apical part of the epithelium (11 min). The redistribution is not always detectable as the orientation of the cell sometimes obscures the apical region (data not shown). Subsequently (25 min), cellular ZO-1 migrates toward the basal pole of the epithelial cell and forms a characteristic funnel shape that can be seen most clearly in en profile view, having a broad base directed toward the apical side of the cell and pointing to its basal pole. In 28 experiments, 15 ± 6 min after the start of apical ZO-1 condensation, the nucleus starts moving apically, to be eventually lost from the epithelium and extruded into the intestinal lumen. This implies that ZO-1 redistribution is the earliest indicator of cell shedding yet identified. Even after the shed nucleus is no longer present in

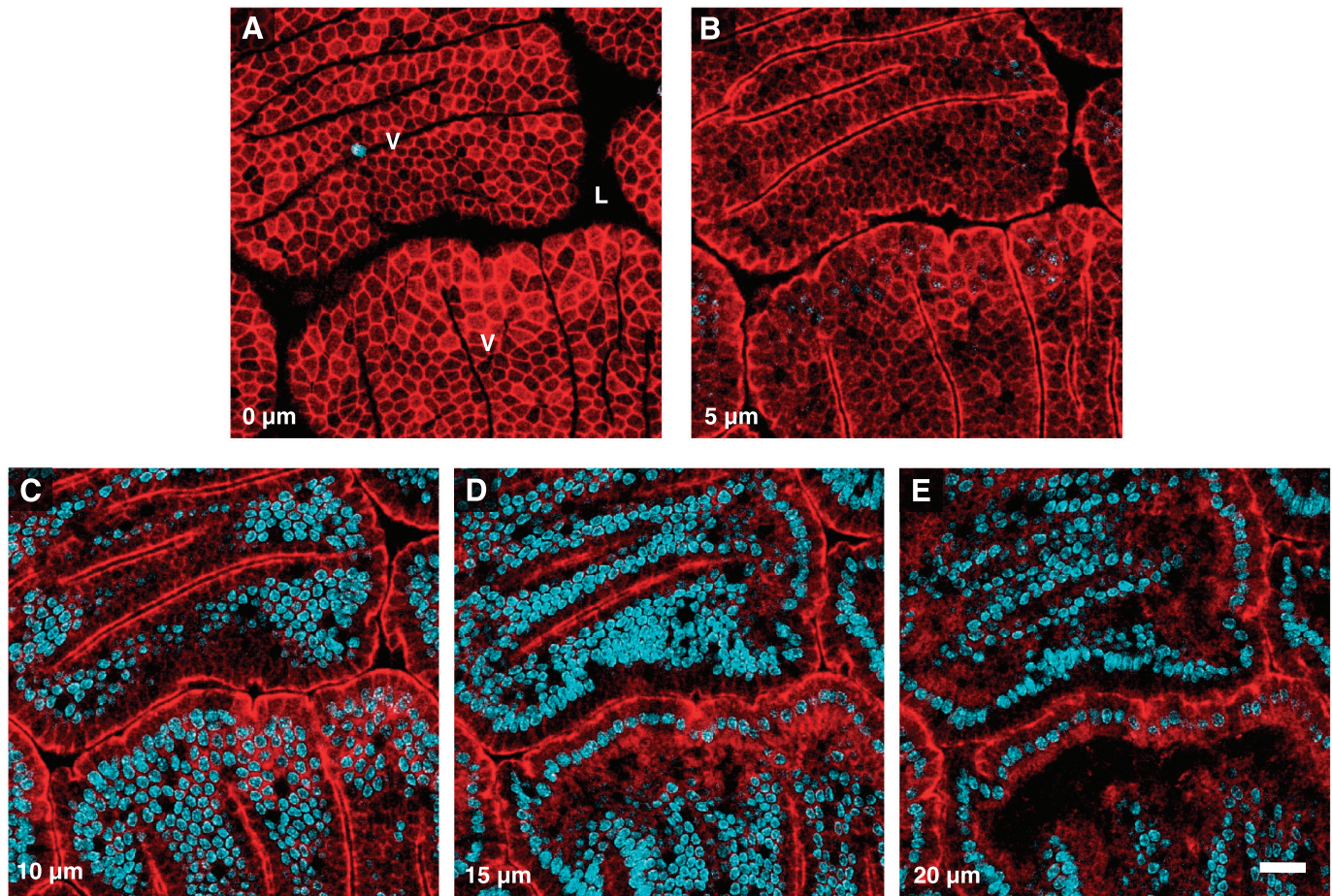


Fig. 1. Confocal microscopy of villi (V) of the mouse jejunum, showing the distribution of the zonula occludens-1 (ZO-1) fusion protein (monomeric red fluorescent protein, mRFP1, red) in the epithelial cell layer, and cell nuclei stained with Hoechst 33342 (blue). ZO-1 can be seen in both en face view (A), where the epithelial cells are cross-sectioned at the surface of the villi, and en profile view (B–E), where the cells are observed from the side, at progressively deeper focus levels, at 5- μm intervals along the Z-axis. L, intestinal lumen. Scale bar = 20 μm .

the images (39–65 min), remaining ZO-1 still stays condensed at the site of shedding.

Figure 3 provides en face views of the same process in a different representative epithelium, displaying a shedding cell (arrow) at multiple time points, and at two Z-axis focal depths. During cell shedding (4–13 min), ZO-1 forms a continuous perimeter encircling the nucleus (a so-called “purse string”), which appeared as a funnel shape in en profile view. This structure likely marks the lateral plasma membrane of the dying cell. After extrusion of the nucleus (≥ 18 min), ZO-1 is still observed as an extended patch that marks the site of cell loss and is visible even focusing into the epithelial layer. These results identify ZO-1 as material that transiently seals the gap that was previously occupied by the shed cell.

As shown in Fig. 3B, the average cell shedding time span can be determined in two ways, with two different markers. Judged by ZO-1 fluorescence, the time span from the initial redistribution of ZO-1 until its condensation at the site of the extruded cell is 45 ± 2 min ($n = 28$). In contrast, the duration reported by nucleus staining (Hoechst 33342) is much shorter (14 ± 1 min), as it begins with first detectable nucleus displacement and ends with completion of cell extrusion into the lumen. Results suggest that before and after a cell has been

extruded from the epithelium, rearrangement of ZO-1 is required.

ZO-1 distribution and gap formation after cell shedding. After a cell has left the epithelium, the residual ZO-1 patch shrinks over time. This is demonstrated qualitatively in Fig. 3 in the progression from 18 to 48 min and analyzed quantitatively in Fig. 4. Measurements were made at the apical boundary of the epithelium (where neighboring cells express normal tight junctions), directly after a cell nucleus detaches from the epithelial layer (0 min) until 20 min later. Figure 4A shows representative images of the ZO-1 patch and surrounding control cells, directly after cell shedding at the site of the patch (0 min) and 16 min later. As shown in the compiled data of Fig. 4B, randomly selected nearby (control) cells maintain a stable size of their boundary with other cells. In contrast, the ZO-1 patch beneath an extruded nucleus initially has a similar size as nonshedding neighbor cells in the monolayer but reduces its size over time. At 16 min after shedding, the average perimeter of the surface area of a ZO-1 patch is $14 \pm 2\%$ of the original value (3.5 ± 0.6 vs. 25 ± 1 μm ; $n = 15$; $P < 0.01$). Measurements of the perimeter of individual cell spaces during the cell shedding process suggest that the cells neighboring the extruding cell do not measurably change size, despite a dra-

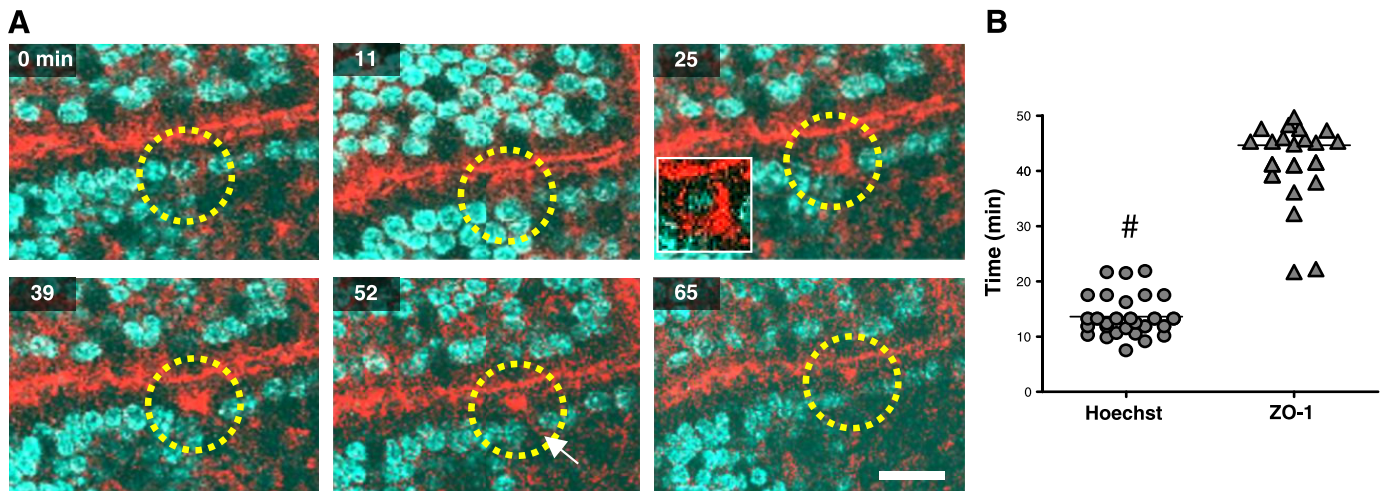


Fig. 2. En profile imaging of cell shedding and ZO-1 redistribution in vivo. *A*: time-course imaging of epithelial villus cell that undergoes extrusion (yellow circle), visualizing mRFP1-ZO-1 (red) and Hoechst 33342 (blue) recorded in en profile view. Apical redistribution of ZO-1 is seen at 11 min, with funnel-shape formation of ZO-1 migrating to the basal pole and engulfing the upward moving cell nucleus at 25 min. Eventually, the epithelial cell is extruded into the lumen, leaving a “gap” behind (white arrow) while remaining ZO-1 appears condensed at the site of shedding (39–65 min). Scale bar = 10 μm . *B*: cell shedding time span measured with Hoechst 33342 (between initiation of cell nucleus migration and extrusion) and ZO-1 (between initial accumulation in the apical cytoplasm and the final apical retention after extrusion). Values are means \pm SE; # $P < 0.001$; $n = 28$ time courses in 18 mice.

matic change in circumference of the region occupied by the shedding cell.

The imaging of ZO-1 during cell shedding enhanced comparison of the residual space (gap) left by a departing cell as detected in both en profile and en face views. When imaging cell shedding in either orientation, measurements of gaps could be made by comparing the dimensions between the neighboring nuclei flanking a shedding cell. Although these dimensions are predicted to be the same (as they should ideally be an equivalent measure in orthogonal planes), Fig. 5*A* shows that the outcomes were different between the two views. The en face view resolved a modest expansion of the shedding cell space during the shedding process (by 23.1%; 9.6 ± 0.3 vs. 7.8 ± 0.3 μm , $n = 26$; $P < 0.01$) and overall reported a larger physical dimension of this space during all measured phases of cell shedding compared with the en profile view. The small size of gaps reported in en profile views (“after”) leads to difficulty in resolving the presence of gaps in this viewing orientation. In both en face and en profile viewing orientations, the space shrinks considerably after cell extrusion by $\sim 40\%$ (7.8 ± 0.3 vs. 4.9 ± 0.2 μm ; $n = 26$; $P < 0.001$) or 65% (5.7 ± 0.3 vs. 2.0 ± 0.2 μm , $n = 19$; $P < 0.001$), respectively. Results are likely explained by the variable angles of optical sectioning that are all designated as “en profile.” En profile views that are even modestly tangential (versus perfectly aligned along the apical-to-basal axis) will incorrectly report smaller dimensions. For example, see Fig. 5*B*. After the nucleus has clearly been shed into the lumen (0 min, see *inset* highlighting ZO-1 funnel in Fig. 5*B*), the remaining gap appears to be small or undetectable at early times when en face viewing reports a readily detected gap (Fig. 4).

Epithelial barrier function relative to ZO-1 during cell extrusion. To test whether ZO-1 redistribution led to loss of epithelial barrier function in the region of a shedding cell, we applied LY to the luminal fluid and evaluated local access of this ~ 450 -molecular weight hydrophilic dye near a shedding cell. As shown in Fig. 6, LY does not penetrate the epithelium

and is excluded from viable cells. During cell shedding, the limit for penetration of the dye was tightly correlated with the location of the redistributed ZO-1. Especially in LY-only images (Fig. 6, *right*) the dynamics of the progressive permeation of LY in the intercellular space around a shedding cell can be clearly appreciated at 27–50 min. It is noteworthy that the permeation of LY into the intercellular space around a shedding cell lags behind the basolateral migration of ZO-1. These data suggest that the observed funnel-shaped (or “purse-string”) ZO-1 configurations are faithful indicators of tight junction location and not signs of dissociation of ZO-1 from an immobile tight junction. Moreover, these observations confirm that LY cannot progress beyond the condensed ZO-1 patch underneath the shedding cell to invade the basolateral spaces of the neighboring epithelium (Fig. 6, 38–50 min). It was observed that ~ 10 min after completion of cell shedding, LY was taken up by shed cells (data not shown), suggesting their membrane permeability became compromised as cell death progressed.

Reaction of neighboring cells to cell shedding. When looking at the experiment depicted in Fig. 6, we noted that the cell neighboring the shedding cell also initiated ZO-1 redistribution. Following up on this observation, we observed that upon extrusion of $\sim 15\%$ (64 of 426) of the epithelial cells, their neighboring epithelial cells also started to be extruded, with a delay of ~ 5 –10 min. For example, in supplemental Fig. S1 (see *AJP-Cell Physiology* website for supplemental figures), *cell 1* initiates the extrusion process manifested by ZO-1 redistribution, purse-string formation, and displacement of the nucleus from the baseline (dotted blue line along the adjacent cell nuclei), eventually leading to cell extrusion by 26 min. Nine minutes after this event, its neighbor *cell 2* starts to shed.

ZO-1, polarized membrane markers, and cell shedding in fixed tissue sections of normal mice. It is possible that the fluorescent (overexpressed) ZO-1 fusion protein behaved abnormally compared with normal ZO-1. Therefore, we performed ZO-1 immunocytochemistry on fixed sections of the

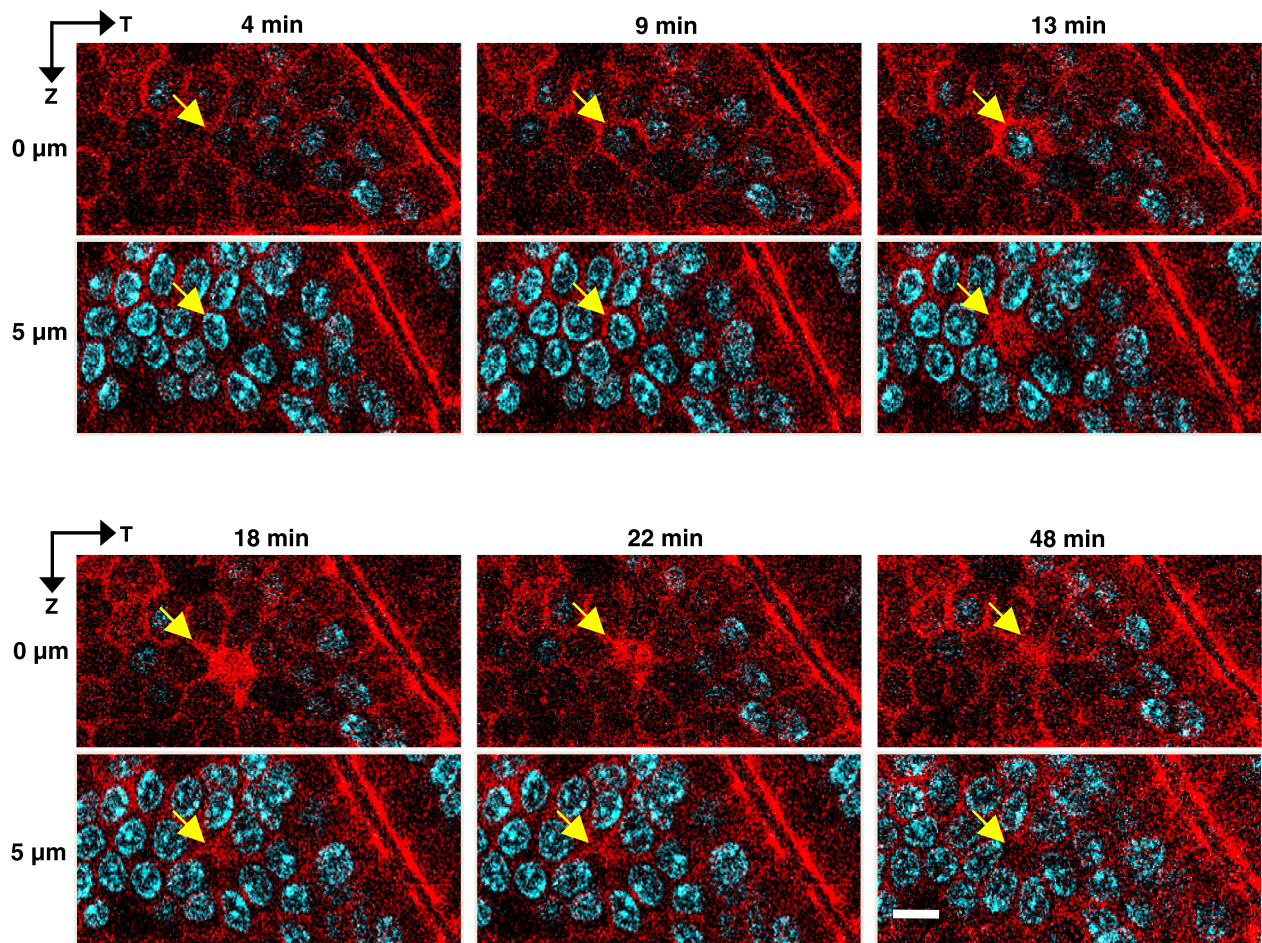


Fig. 3. En face imaging of cell shedding and ZO-1 redistribution in vivo. Time-course imaging of the fate of a shedding epithelial cell (arrow) in en face view at multiple time points and at two Z-axis focal depths (0 and 5 μm), revealing shedding while ZO-1 encircles the nucleus (9–13 min) and residual ZO-1 accumulation is visible in the epithelial layer after cell extrusion (≥ 18 min) as an extended patch that marks the site of cell loss. The ZO-1 patch shrinks over time. Scale bar = 5 μm .

small intestine from normal mice. Although cell shedding structures are not abundant in such sections (3), we identified sites with shedding nuclei and found clear hallmarks of altered ZO-1 distribution, similar to those reported in the transgenic mouse studies. These included the appearance of a funnel-shaped ZO-1 distribution associated with modestly displaced nucleus position as must occur in early phases of shedding (Fig. 7A) and a patch of ZO-1 remaining in the space vacated by extruded cells (Fig. 7, C and D). Actin counterstaining marks predominately cell membranes (apical membranes in healthy cells and cells in early shedding phase) and helps demonstrate that the ZO-1 patches (Fig. 7, B–D) fill the gap left behind by the extruded cell. Diffuse and diminished ezrin positivity was noted at the apical boundary of shedding cells, but no ezrin was detected in the basolateral membranes (Fig. 8A). Conversely, the E-cadherin at the basolateral membrane of shedding cells colocalized with ZO-1 in the funnel shape but was not observed in the apical membrane (Fig. 8B).

DISCUSSION

Renewal of the intestinal epithelium is a consequence of the short lifetime and rapid production of intestinal epithelial cells, resulting in frequent cell shedding from the

intestinal villus. This report evaluates physiological cell shedding in the mouse jejunal epithelium, intentionally avoiding pharmacological and mechanical manipulation, so that the baseline events can be characterized before comparison with the stimulated cell shedding observed in disease (16, 20). As will be discussed below the results demonstrate that redistribution of ZO-1 serves as an early marker of cell shedding as well as a marker of the movement of tight junctions that sustain continual epithelial barrier function during cell extrusion.

Duration and progression of the cell shedding process. Intravital confocal imaging of a fluorescent ZO-1 fusion protein shows that the process of cell shedding in the mouse jejunum starts 15 min before any detectable motion of the cell nucleus from the epithelial layer, and healing of the monolayer continues at least 15 min after the cell is lost from the epithelium. After initial redistribution of ZO-1, the cell extrusion process starts, lasting ~ 13 min, while the nucleus appears engulfed in a characteristic funnel cone of ZO-1 protein. Our observations confirm that an epithelial cell destined to be shed does not yet undergo nuclear chromatin condensation (35) but reveal that this hallmark of apoptosis is visible directly after cells leave the monolayer (supplemental Fig. S2), and we have

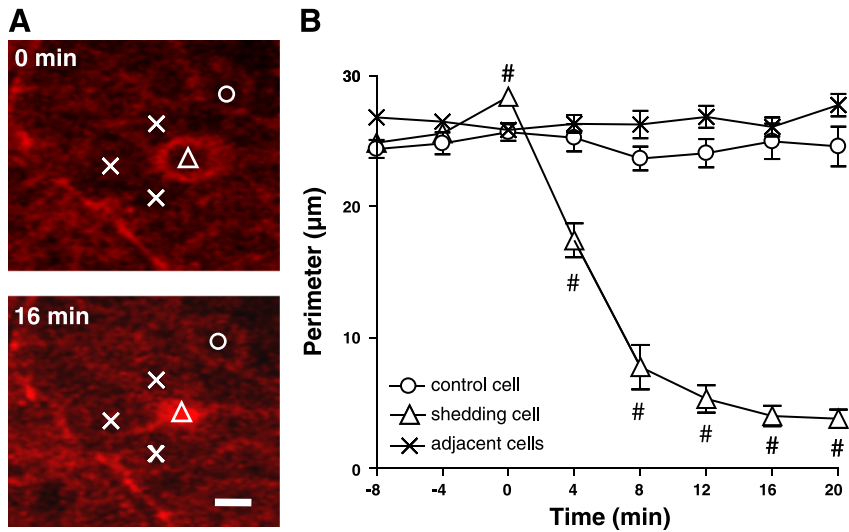


Fig. 4. Time course of gap resolution after cell shedding. A: representative images directly after cell shedding at 0 min, and 16 min later. Symbols mark site of the ZO-1 patch (open triangle), surrounding cells directly adjoining the shedding site (X) and more distant control cell (open circle). Scale bar = 5 μm. B: measurements from multiple experiments at the apical boundary of the epithelium (where neighboring cells express normal tight junctions). Symbols are the same as in A. Time 0 is defined as the time of losing a cell nucleus from the epithelial layer. ZO-1 patch is reduced in size over time (#*P* < 0.01 vs. adjacent cells at same time point; *n* = 15).

reported previously such condensation is routinely observed in dead cells within the intestinal lumen (35). Recently we showed that TNF-α-induced shedding is inhibited by the caspase inhibitor Q-VD-OPh (37). A similar use of inhibitors in the current work would be extremely difficult due to the low frequency of unstimulated shedding. Since chromatin condensation occurs late in apoptosis, it remains unknown whether earlier events in apoptosis (e.g., mitochondrial dysfunction, caspase activation) start coincident with the early redistribution of ZO-1 that starts in advance of cell extrusion (3). At present, altered ZO-1 distribution provides the earliest and latest hallmark of cell shedding in the epithelial layer.

The tight junction may be an active participant in catalyzing cell extrusion. Multicellular wounds heal by a variety of different mechanisms, including circumferential contraction of an actomyosin purse string resembling the funnel-shaped ZO-1 configuration seen in our preparations, which assembles around wound borders and is dependent on the small GTPase Rho (2, 25). Indeed, cell shedding is inhibited by genetic deletion of myosin light chain kinase (37). Results in Figs. 4 and 5 suggest that changes in shape and size of shedding cells are more prominent than any changes in surrounding cells within the epithelial layer. The constancy of the cells neighboring the extruding cell does not support the idea that the

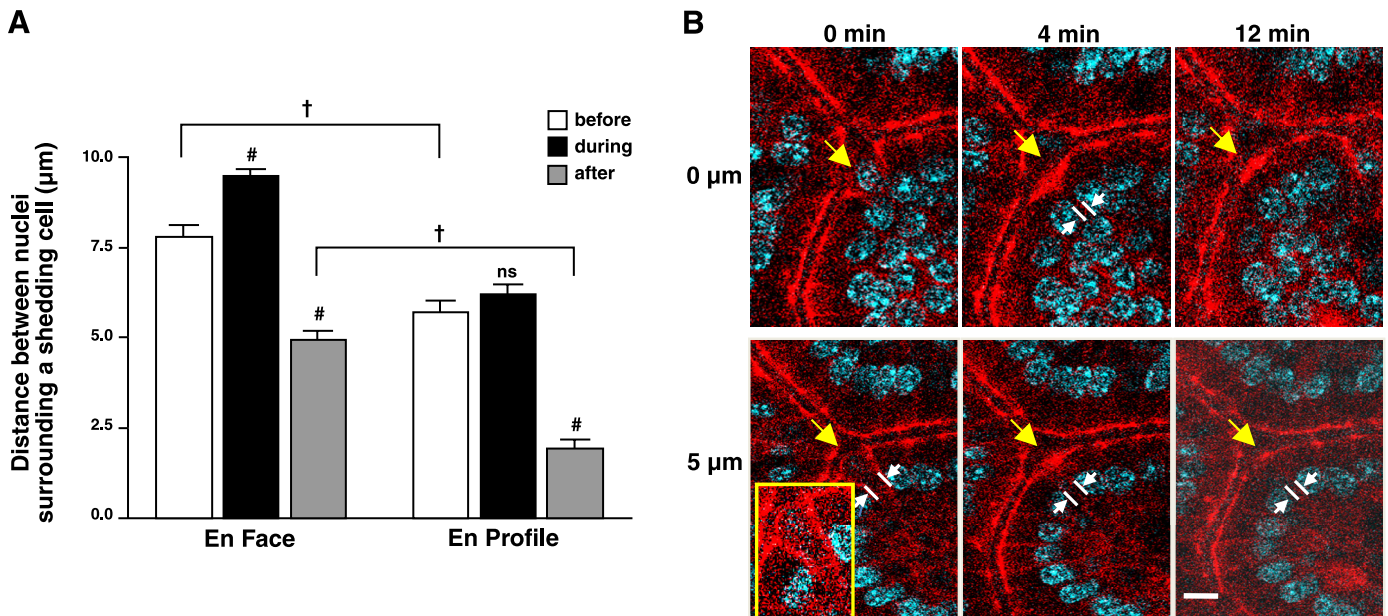


Fig. 5. Comparison of en face and en profile measures of the space (gap) in the epithelial layer resulting from cell shedding. Cell nuclei were stained with Hoechst 33342. A: measurements made of the distance between the epithelial cell nuclei that are on either side flanking a shedding cell before, during, and after cell extrusion. In en face views, measured as linear distance between nuclei averaging values from three lines each crossing the center of the shedding cell to intersect a pair of nuclei in different flanking cells. In en profile view, measured as linear distance between the two nuclei flanking the shedding cell (as highlighted in B). Comparisons to the “before” condition in the same viewing orientation: ns, not significant. #*P* < 0.001, comparisons between viewing orientation in same time category; †*P* < 0.001. (*n* = 45 in total). B: yellow arrow identifies shedding cell in en profile view, and white lines and arrows demarcate distance between flanking nuclei surrounding the shedding cell. Inset: highlight of ZO-1 funnel.

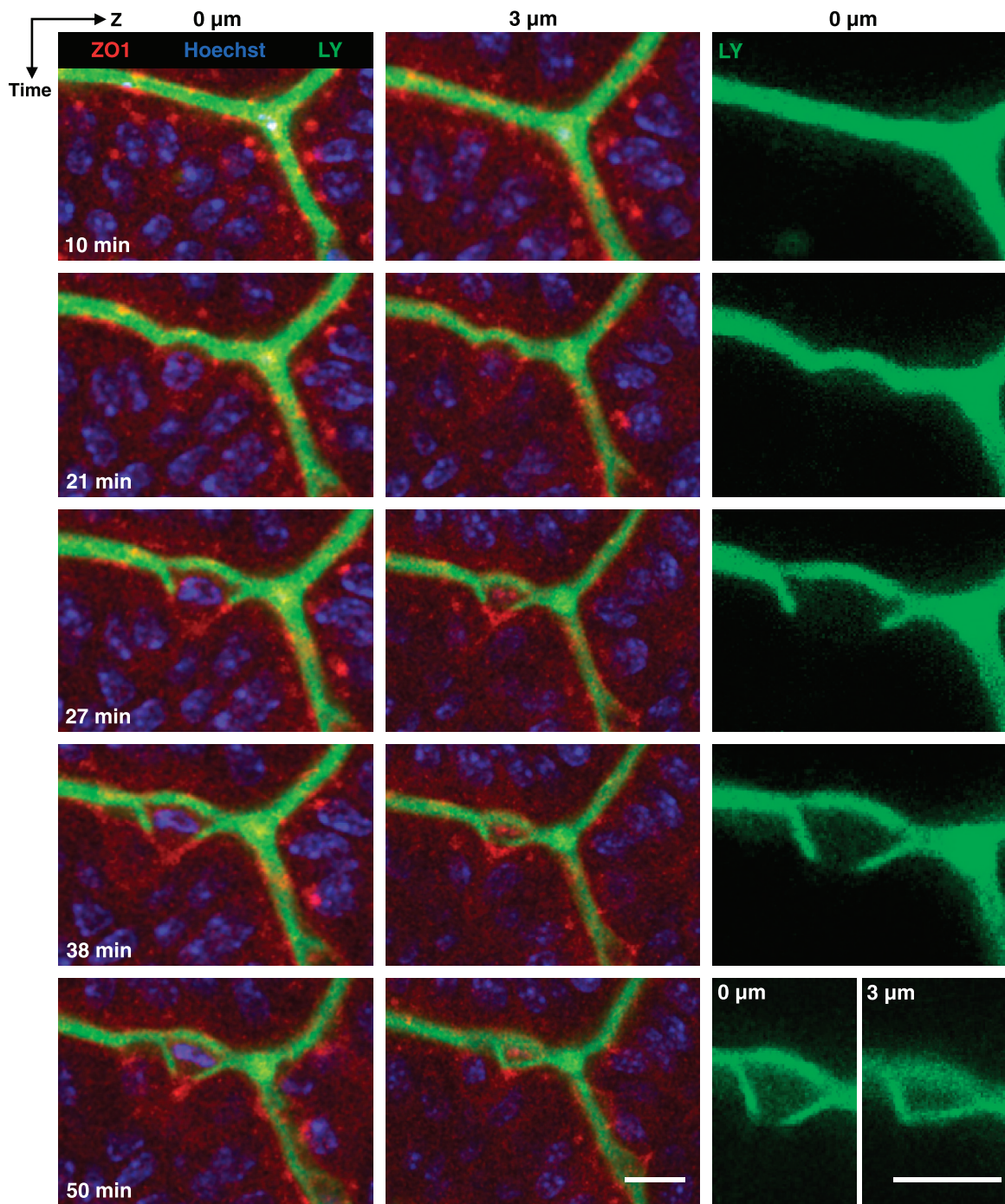


Fig. 6. Testing local permeability at sites of cell shedding using luminal Lucifer Yellow (LY). Images of Hoechst 33342 (blue), ZO-1 (red), and LY fluorescence (green) collected at indicated time points in a representative experiment. Each row of images are collected at a single time point. *Left* and *middle*, results overlaying all fluorescent reporters at two Z-axis focal depths (0 and 3 μm , respectively). *Right*, LY fluorescence alone (0 μm). LY fills the luminal space between villi, and the intercellular space progressing around the lateral sides of the shedding cell. Limit of LY permeation is always defined by site of condensed ZO-1 underneath the shedding cell. Scale bar = 5 μm .

neighboring cells produce local force to push the shedding cell out, although this possibility cannot be fully ruled out on the basis of our measurements. Alternatively, we speculate that the ventrally migrated ZO-1 may be bound to both the basolateral membrane and the epithelial cell cytoskeleton, and contraction of the cytoskeletal elements in the shedding cell might produce force that acts to pull up the cell and extrude it. This sequence

of events, as depicted as a model in supplemental Fig. S3, awaits further experimental proof.

Detection and fate of gaps. The presence of discontinuities in the intestinal epithelium was reported previously by us and others (16, 21, 35–37), but the variable recognition and uncertain fate of gaps have remained problematic. The variable recognition may be largely due to the way gaps have been

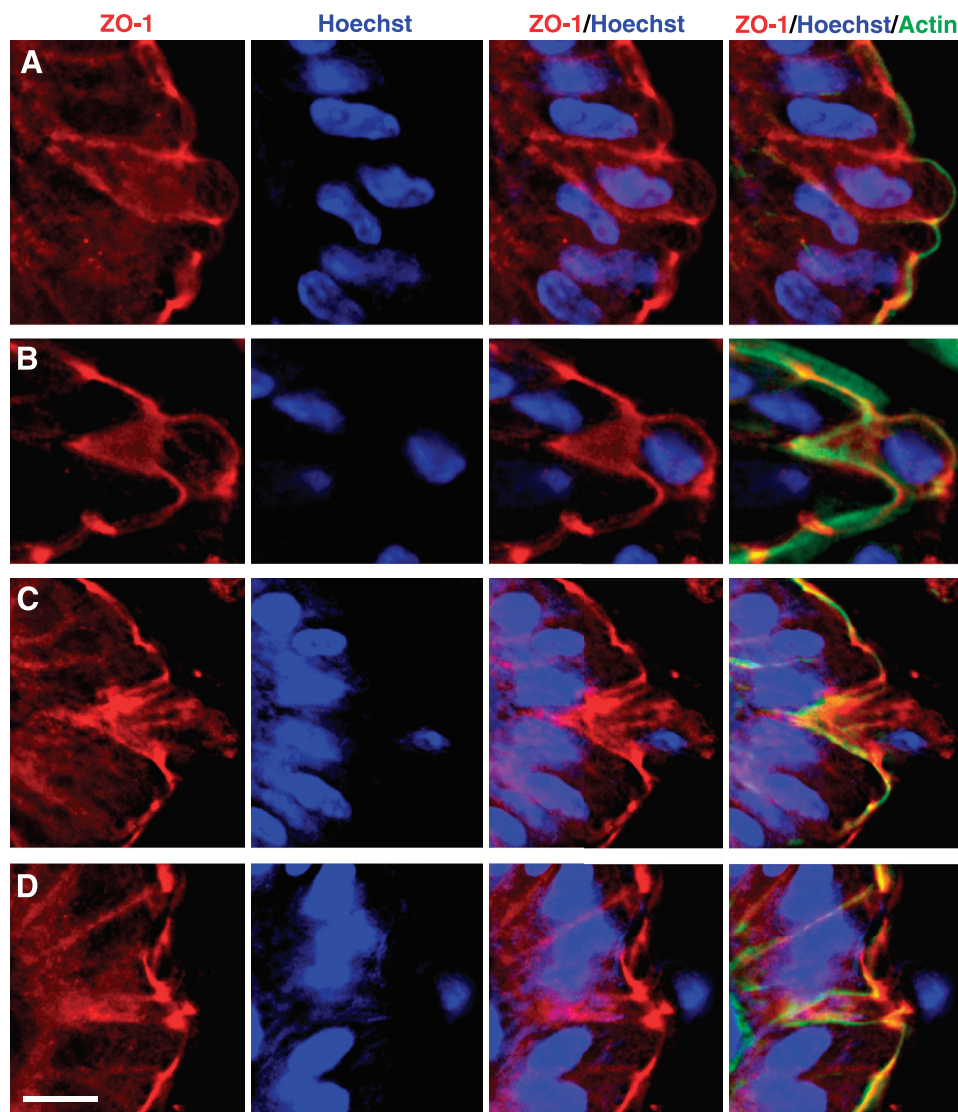


Fig. 7. Immunofluorescence staining of ZO-1 in shedding cells from normal mouse jejunum. As described in MATERIALS AND METHODS, fixed tissue sections were stained for ZO-1 (red), actin (green), and cell nucleus (Hoechst, blue) and imaged by fluorescence microscopy. The figure shows results from four separate stages (A–D) in which a Hoechst-stained cell nucleus was observed to be displaced from neighbors in the process of cell shedding. Each A–D panel shows a series of images to highlight (from left to right) ZO-1, Hoechst, ZO-1/Hoechst overlay, and ZO-1/Hoechst/actin overlay. Scale bar = 10 μ m.

studied in the light microscope. Although gaps are readily seen in en face view, gaps can be misidentified or hardly visible in en profile view. Direct measurements after shedding suggest that this is likely due to the variable viewing angle of en profile evaluations. A second confounder is that static studies of the epithelium (versus direct evaluation of a shedding cell) can be deceiving. In prior work, some gaps were misidentified in static images due to an unexpected resistance of some (goblet) cell nuclei to vital staining by Hoechst 33258 compared with Hoechst 33342 (likely because the latter stain has additional ethyl groups that render it more lipophilic) (13). Examples of this differential staining are shown in supplemental Fig. S4. Directly comparing images from these two DNA stains indicates that the previously reported $\sim 3\%$ cell positions at the villus tip being occupied by gaps in the steady state (35) represented an overestimation by approximately fourfold (data not shown).

Our observations with ZO-1, in a setting of only evaluating the consequences of a confirmed cell extrusion event, show that gaps are formed and are resolved shortly after cell shedding. The gap resulting from shedding includes a patch of

residual ZO-1 remaining after cell extrusion, which shrinks in size by about two-thirds within minutes after cell loss. The cell source of the ZO-1 patch remains unknown but since the shed cell is impermeable to extracellular LY at the time of shedding, it is likely to be from the cells neighboring the shed cell. This is difficult to resolve with the lack of cytoplasm found in gaps defined by multiple vital stains (16, 35) and the open space between the ZO-1 on lateral membranes of adjacent cells. In his speculative working model of the cell extrusion process, constructed on the basis of static pictures from freeze-fracture, light, and electron microscope studies on villus tip extrusion zones in rats and hamsters, Madara (18) proposed that newly formed tight junction elements “zipper” the epithelium closed as extrusion proceeds, thus preventing epithelial discontinuities from occurring. As shown in supplemental Fig. 3, from our in vivo studies, we hypothesize that protrusions with ZO-1 attachment are restricted to the area directly beneath the shedding cell until the gap closes over 20 min postcell extrusion.

ZO-1 redistribution in the normal mouse. We have studied living tissue to be able to fully appreciate the temporal and

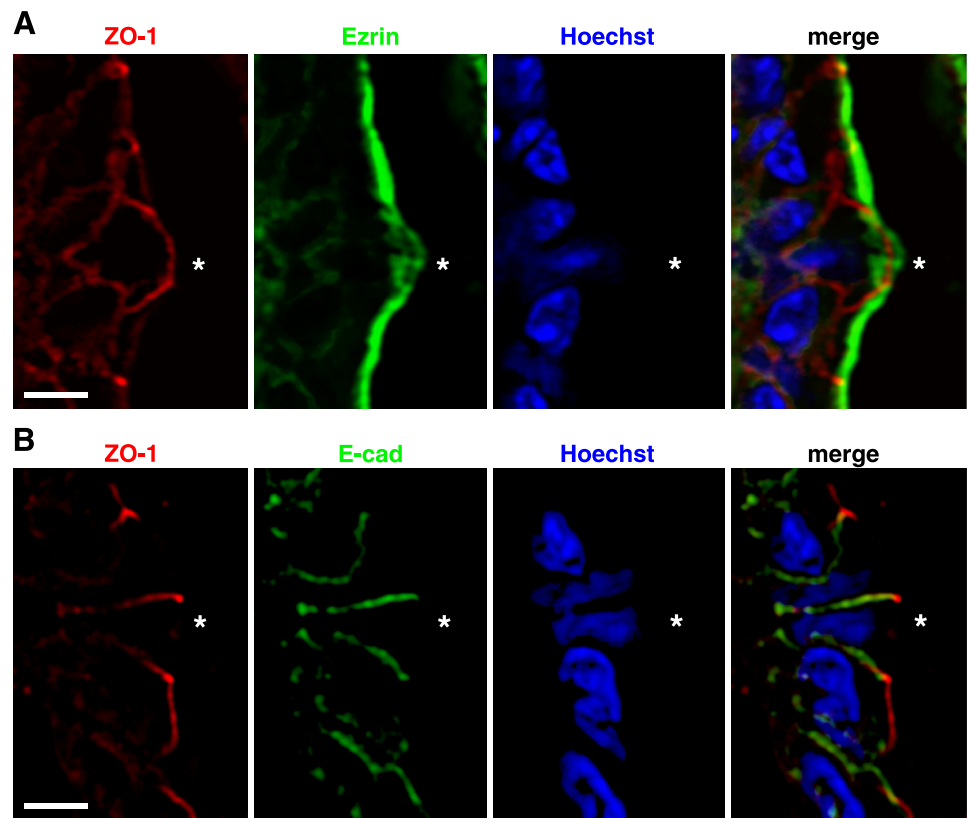


Fig. 8. Immunofluorescence staining of ezrin (A) and E-cadherin (B) in shedding cells from normal mouse jejunum. Fixed tissue sections were stained for ZO-1 (red), ezrin or E-cadherin (green), and Hoechst (blue) and imaged by fluorescence microscopy. *shedding cell. Scale bar = 10 μ m.

spatial aspects of cell shedding in a physiological setting. In our study, transgenic mice overexpressing a ZO-1 fusion protein were used to learn by inference about the dynamics of normal ZO-1 (20, 27). To address concerns about potential artifacts due to overexpression of ZO-1 or use of the fluorescent protein tag, we performed immunofluorescence staining of the normal mouse. Our previous studies using fixed tissue sections of wild-type mice had proven to be inconclusive about ZO-1 distribution in shedding cells. We previously obtained an indication that ZO-1 might play a dynamic role in cell renewal, as shedding cells were observed to be bounded by neighboring cells contacting at the basal pole in a V-shaped formation, with a spot of ZO-1 immunoreactivity at the base of the V (3, 35). However, since this phenomenon was observed in only 9% of identified shedding cells and the remaining cells had no detectable points of ZO-1-immunoreactivity near the basement membrane, we concluded that tight junctions formed by the cells neighboring a shedding cell could only be used in a fraction of instances to help reseal a breach in the epithelial layer (35). In the present study, we used a more sensitive immunofluorescence method to visualize ZO-1 in fixed tissue sections versus our prior use of the peroxidase histochemical detection system (3, 35). Although fixed tissue could not give information about the temporal aspects of ZO-1 dynamics, it did reveal ZO-1 spatial redistribution during phases of epithelial cell shedding that could be recognized in fixed sections: lateral formation around the cell nucleus in early shedding and filling of the remaining gap at late phases of cell extrusion. Therefore, there is a solid parallel between the data obtained from both normal ZO-1 and from the fluorescent ZO-1 fusion protein.

Epithelial barrier function is maintained during cell shedding. The epithelial barrier function is sustained at the apical pole of the intestinal epithelial layer despite apparent discontinuities in this layer (18, 35). Here we have monitored epithelial barrier function using the plasma-membrane impermeant LY and related this in real-time to the process of cell extrusion and ZO-1 redistribution. The results clearly show that epithelial cell barrier function is maintained throughout the cell extrusion process. Although LY starts modestly invading the lateral intercellular spaces surrounding a shedding cell, LY does not penetrate the epithelium nor enter the shedding cell itself. The LY penetration data indicate that the epithelial barrier moves to the lateral membranes of the epithelial cell during shedding, suggesting that the redistributed ZO-1 is part of a larger coordinated movement of multiple junctional proteins in both a shedding cell and its neighbors. This is supported by the independent observation that at least one component of the adherens junction (E-cadherin) also colocalizes with the redistributed ZO-1 during shedding. In TNF- α -induced shedding, claudin 7 and 15, occludin, and E-cadherin are all redistributed into a funnel during shedding (37). In this way, further penetration of LY is prevented and the barrier function of the epithelium maintained.

Results suggest alterations occur in both apical and basolateral membrane structures during shedding but do not demonstrate any mislocalization of (two tested) polarized proteins at opposing membrane domains despite a broad redistribution of ZO-1 (Fig. 8). This suggests that cell shedding does not lead to gross mixing of apical and basolateral membrane proteins in either shed cells or their immediate neighbors. Colocalization of E-cadherin with the redistributed ZO-1 suggests that both

adherens and tight junction proteins may be redistributed during the cell shedding process.

Reaction of neighboring epithelial cells to cell shedding. Irrespective the role of neighboring cells in sealing gaps and pushing out of a shedding cell, these cells very soon become shed themselves. Our finding that this secondary shedding follows that of the initial shedding cell with a rather fixed delay (~5–10 min) strongly suggests that shedding epithelial cells induce the shedding of their neighbors by some kind of direct, local communication. Clearly, this communication would seem different from the signal a cell destined for apoptosis would send to neighboring epithelial cells to start its own extrusion process (25). The regulation of gap junctional intercellular communication in the intestine is not well understood. Cytokines produced by epithelial cells (31) are possible candidates, whereas recently a novel physiological link was described between Toll-like receptor TLR2 and gap junctional intercellular communication through modulation of connexin-43 during acute and chronic inflammatory injury of the intestinal epithelial cell barrier (6). Whether TLR2 and connexin-34, in addition to ZO-1, are involved in the presently described shedding-induced neighboring cell extrusion and in a manner compatible with the proposed dynamic model of proliferation and differentiation in the intestinal crypt based on the secretion of a hypothetical intraepithelial factor (9), remains to be established.

Our results from high-resolution intravital three-dimensional microscopy reveal linkage between two characteristics of physiological cell shedding: redistribution of the tight junction protein ZO-1 and cell extrusion from the epithelium. These processes lead to the formation of an epithelial gap that is resolved in the 20 min after cell extrusion. During all phases of the cell extrusion and epithelial repair process, barrier function is sustained. ZO-1 redistribution is the earliest event yet identified as a herald of physiological epithelial cell shedding, and sliding of tight junction function along the lateral plasma membrane is an important aspect of sustaining barrier function during epithelial cell renewal. Our study provides the basis for future investigations where (aberrant) ZO-1 redistribution may be a key event in diseases caused by mechanical, inflammatory, or bacterial stresses (22) to the mucosal epithelial barrier.

ACKNOWLEDGMENTS

We thank Dr. Andrea Matthis for breeding and maintaining the transgenic mouse colony and Chet Closson for technical support in confocal microscopy.

GRANTS

The study received funding through NIH Grants R21DK074976 (to M. H. Montrose) and R01DK61931 and R01DK68271 (to J. R. Turner), and Wellcome Trust Grant WT087768AIA (to A. J. M. Watson).

DISCLOSURES

No conflicts of interest, financial, or otherwise are declared by the author(s).

REFERENCES

1. **Baron DA, Miller DH.** Extrusion of colonic epithelial cells in vitro. *J Electron Microscop Tech* 16: 15–24, 1990.
2. **Bement WM, Mandato CA, Kirsch MN.** Wound-induced assembly and closure of an actomyosin purse string in *Xenopus* oocytes. *Curr Biol* 9: 579–587, 1999.
3. **Bullen TF, Forrest S, Campbell F, Dodson AR, Hershman MJ, Pritchard DM, Turner JR, Montrose MH, Watson AJ.** Characterization of epithelial cell shedding from human small intestine. *Lab Invest* 86: 1052–1063, 2006.
4. **Chen L, Park SM, Turner JR, Peter ME.** Cell death in the colonic epithelium during inflammatory bowel diseases: CD95/Fas and beyond. *Inflamm Bowel Dis* 16: 1071–1076.
5. **Clark AG, Miller AL, Vaughan E, Yu HY, Penkert R, Bement WM.** Integration of single and multicellular wound responses. *Curr Biol* 19: 1389–1395, 2009.
6. **Ey B, Eykling A, Gerken G, Podolsky DK, Cario E.** TLR2 mediates gap junctional intercellular communication through connexin-43 in intestinal epithelial barrier injury. *J Biol Chem* 284: 22332–22343, 2009.
7. **Fanning AS, Jameson BJ, Jesaitis LA, Anderson JM.** The tight junction protein ZO-1 establishes a link between the transmembrane protein occludin and the actin cytoskeleton. *J Biol Chem* 273: 29745–29753, 1998.
8. **Furuse M.** Molecular basis of the core structure of tight junctions. *Cold Spring Harb Perspect Biol* 2: a002907.
9. **Gerike TG, Paulus U, Potten CS, Loeffler M.** A dynamic model of proliferation and differentiation in the intestinal crypt based on a hypothetical intraepithelial growth factor. *Cell Prolif* 31: 93–110, 1998.
10. **Groschwitz KR, Ahrens R, Osterfeld H, Gurish MF, Han X, Abrink M, Finkelman FD, Pejler G, Hogan SP.** Mast cells regulate homeostatic intestinal epithelial migration and barrier function by a chymase/Mcpt4-dependent mechanism. *Proc Natl Acad Sci USA* 106: 22381–22386, 2009.
11. **Guan Y, Dong J, Tackett L, Meyer JW, Shull GE, Montrose MH.** NHE2 is the main apical NHE in mouse colonic crypts but an alternative Na⁺-dependent acid extrusion mechanism is upregulated in NHE2-null mice. *Am J Physiol Gastrointest Liver Physiol* 291: G689–G699, 2006.
12. **Guan Y, Worrell RT, Pritts TA, Montrose MH.** Intestinal ischemia-reperfusion injury: reversible and irreversible damage imaged in vivo. *Am J Physiol Gastrointest Liver Physiol* 297: G187–G196, 2009.
13. **Hawley R, Hawley T.** Flow cytometry protocols. In: *Molecular Biology*, edited by Clifton N. Totowa, NY: Humana, 2004.
14. **Inagaki-Tachibana E, Natori Y, Hayashi H, Suzuki Y.** In vitro diffusion barriers of the mouse jejunum in Ussing chambers. *J Nutr Sci Vitaminol (Tokyo)* 54: 30–38, 2008.
15. **Jinguji Y, Ishikawa H.** Electron microscopic observations on the maintenance of the tight junction during cell division in the epithelium of the mouse small intestine. *Cell Struct Funct* 17: 27–37, 1992.
16. **Kiesslich R, Goetz M, Angus EM, Hu Q, Guan Y, Potten C, Allen T, Neurath MF, Shroyer NF, Montrose MH, Watson AJ.** Identification of epithelial gaps in human small and large intestine by confocal endomicroscopy. *Gastroenterology* 133: 1769–1778, 2007.
17. **Lipkin M.** Proliferation and differentiation of normal and diseased gastrointestinal cells. In: *Physiology of the Gastrointestinal Tract*, edited by Johnson L. NY: Raven, 1987, p. 255–284.
18. **Madara JL.** Maintenance of the macromolecular barrier at cell extrusion sites in intestinal epithelium: physiological rearrangement of tight junctions. *J Membr Biol* 116: 177–184, 1990.
19. **Marchiando AM, Graham WV, Turner JR.** Epithelial barriers in homeostasis and disease. *Annu Rev Pathol* 5: 119–144, 2010.
20. **Marchiando AM, Shen L, Graham WV, Weber CR, Schwarz BT, Austin JR, 2nd Raleigh DR, Guan Y, Watson AJ, Montrose MH, Turner JR.** Caveolin-1-dependent occludin endocytosis is required for TNF-induced tight junction regulation in vivo. *J Cell Biol* 189: 111–126, 2010.
21. **Moore R, Carlson S, Madara JL.** Villus contraction aids repair of intestinal epithelium after injury. *Am J Physiol Gastrointest Liver Physiol* 257: G274–G283, 1989.
22. **Pentecost M, Otto G, Theriot JA, Amieva MR.** *Listeria monocytogenes* invades the epithelial junctions at sites of cell extrusion. *PLoS Pathog* 2: e3, 2006.
23. **Potten CS, Owen G, Roberts SA.** The temporal and spatial changes in cell proliferation within the irradiated crypts of the murine small intestine. *Int J Radiat Biol* 57: 185–199, 1990.
24. **Rao RK, Basuroy S, Rao VU, Karnaky KJ Jr, Gupta A.** Tyrosine phosphorylation and dissociation of occludin-ZO-1 and E-cadherin-beta-catenin complexes from the cytoskeleton by oxidative stress. *Biochem J* 368: 471–481, 2002.
25. **Rosenblatt J, Raff MC, Cramer LP.** An epithelial cell destined for apoptosis signals its neighbors to extrude it by an actin- and myosin-dependent mechanism. *Curr Biol* 11: 1847–1857, 2001.

26. **Russo JM, Florian P, Shen L, Graham WV, Tretiakova MS, Gitter AH, Mrsny RJ, Turner JR.** Distinct temporal-spatial roles for rho kinase and myosin light chain kinase in epithelial purse-string wound closure. *Gastroenterology* 128: 987–1001, 2005.
27. **Shen L, Turner JR.** Actin depolymerization disrupts tight junctions via caveolae-mediated endocytosis. *Mol Biol Cell* 16: 3919–3936, 2005.
28. **Shen L, Weber CR, Turner JR.** The tight junction protein complex undergoes rapid and continuous molecular remodeling at steady state. *J Cell Biol* 181: 683–695, 2008.
29. **Slattum G, McGee KM, Rosenblatt J.** P115 RhoGEF and microtubules decide the direction apoptotic cells extrude from an epithelium. *J Cell Biol* 186: 693–702, 2009.
30. **Snedecor G, Cochran W.** *Statistical Methods*. Ames, IA: Iowa State University Press, 1989.
31. **Stadnyk AW.** Intestinal epithelial cells as a source of inflammatory cytokines and chemokines. *Can J Gastroenterol* 16: 241–246, 2002.
32. **Stevenson BR, Siliciano JD, Mooseker MS, Goodenough DA.** Identification of ZO-1: a high molecular weight polypeptide associated with the tight junction (zonula occludens) in a variety of epithelia. *J Cell Biol* 103: 755–766, 1986.
33. **Turner JR, Rill BK, Carlson SL, Carnes D, Kerner R, Mrsny RJ, Madara JL.** Physiological regulation of epithelial tight junctions is associated with myosin light-chain phosphorylation. *Am J Physiol Cell Physiol* 273: C1378–C1385, 1997.
34. **Walker W.** Intestinal transport of macromolecules. In: *Physiology of the Gastrointestinal Tract*, edited by Johnson LR. NY: Raven, 1981, p. 1271–1286.
35. **Watson AJ, Chu S, Sieck L, Gerasimenko O, Bullen T, Campbell F, McKenna M, Rose T, Montrose MH.** Epithelial barrier function in vivo is sustained despite gaps in epithelial layers. *Gastroenterology* 129: 902–912, 2005.
36. **Watson AJ, Duckworth CA, Guan Y, Montrose MH.** Mechanisms of epithelial cell shedding in the Mammalian intestine and maintenance of barrier function. *Ann NY Acad Sci* 1165: 135–142, 2009.
37. **Marchiando AM, Shen L, Graham WV, Edelblum KL, Duckworth CA, Guan Y, Montrose MH, Turner JR, Watson AJ.** The epithelial barrier is maintained by in vivo tight junction expansion during pathologic intestinal epithelial shedding. *Gastroenterology* 2011 January 13.

